Lawrence Berkeley National Laboratory
Recent Work

Title

PHOTOIONIZATION STUDIES OF THE HETERONUCLEAR RARE GAS VAN DER WAALS MOLECULES XeKr, XeAr AND KrAr

Permalink

https://escholarship.org/uc/item/8gs3z34k

Author

Ng, C.Y.

Publication Date

1977-02-01

PHOTOIONIZATION STUDIES OF THE HETERONUCLEAR RARE GAS VAN DER WAALS MOLECULES XeKr, XeAr AND KrAr

C. Y. Ng, P. W. Tiedemann, B. H. Mahan, and
Y. T. Lee

February 1977

DISCLAIMER

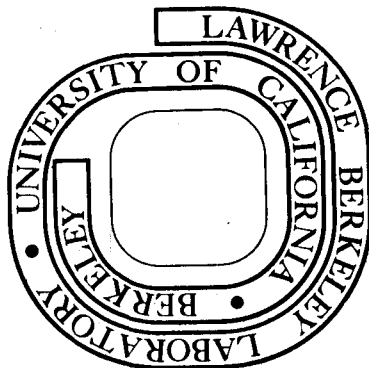PHOTOIONIZATION STUDIES OF THE HETERONUCLEAR RARE GAS
VAN DER WAALS MOLECULES XeKr, XeAr and KrAr

C. Y. Ng, P. W. Tiedemann, B. H. Mahan and Y. T. Lee

Materials and Molecular Research Division
Lawrence Berkeley Laboratory

and

Department of Chemistry
University of California
Berkeley, California 94720

ABSTRACT

The photoionization efficiency curves of the heteronuclear rare

gas van der Waals molecules XeKr, XeAr and KrAr were obtained with

the molecular beam technique in the wavelength range from 790 to

1065 Å (11.64 - 15.69 eV). The ionization potentials were found

to be 11.757 ± 0.017 eV for XeKr, 11.985 ± 0.017 eV for XeAr, and

13.425 ± 0.020 eV for KrAr. From the known dissociation energies

of the ground state XeKr, XeAr and KrAr van der Waals molecules as

determined by low energy molecular beam elastic scattering experiments,

the binding energies for the ground state of the heteronuclear rare

gas molecular ions were deduced to be 0.37 ± 0.02 eV for $XeKr^+$,

0.14 ± 0.02 eV for $XeAr^+$, and 0.59 ± 0.02 eV for $KrAr^+$. The photoion

spectra of the heteronuclear rare gas dimers, R_1R_2, exhibit prominent

autoionization structure which is found to correlate very well with

the excited molecular Rydberg states, $R_1^*R_2$ and $R_1R_2^*$, formed by the

interaction of a normal ground state rare gas atom, R_1 (or R_2), and

an excited atom, R_2^* (or R_1^*), in the $n'p^5(^2P_{1/2, \, 3/2})ns$ (nd) configuration (where $n' = 3$ for Ar, $n' = 4$ for Kr, and $n' = 5$ for Xe). The excitation of XeKr, XeAr and KrAr is found to obey the parity selection rule, $\Delta\ell = \pm 1$, in agreement with previous experimental observation in the photoionization studies of Kr_2 and Ar_2. The Rydberg series $5p^2(^2P_{1/2})ns$ (nd) for Xe, and $4p^5(^2P_{1/2})ns$ (nd) for Kr, which is manifested as auto-ionization lines in the photoion spectra of the van der Waals rare gas dimers XeAr and XeKr respectively, were red shifted with respect to the positions in the photoionization efficiency curves of Xe and Kr. This allows one to calculate the potential energy for the excited molecular Rydberg state at a distance which corresponds to the equilibrium interatomic distance of the ground state van der Waals molecule. For $Xe(5p^5(^2P_{1/2})ns$ (nd)) $+ Ar(^1S_0)$ one obtains 0.06 eV and for $Xe(^1S_0) + Kr(4p^5(^2P_{1/2})ns$ (nd)), 0.10 eV. These values are found to be in agreement with what one would expect from a charge induced-dipole interaction.

INTRODUCTION

One of the methods of determining the binding energy between a rare gas atom R_1 and a rare gas atomic ion R_2^+ is low energy ion-atom elastic differential scattering cross section measurements. This method relies on the identification of the rainbow angle and the fitting of the elastic differential scattering cross section at many different collisional energies with an assumed parametrized potential. There are many difficulties which limit the accuracy of the potential obtained in this way. First, it is difficult to produce a low energy ion beam of less than a few electron volts with narrow energy spread and having enough intensity for the differential scattering measurements. Second, even if a pure ground state atomic ion beam ($^2P_{3/2}$) can be produced, the differential scattering pattern is still the result of the interference from several potential energy surfaces. The data fitting is thus by no means a trivial problem.

The lower bound for the dissociation energy of ground state rare gas diatomic molecular ions $(R_1R_2)^+$ can also be determined by finding the threshold energy for the electron or photon induced associative ionization process, $R_1^* + R_2 \rightarrow (R_1R_2)^+ + e$ along with the ionization potential of R_1. The mechanism of producing $(R_1R_2)^+$ involves a resonant excitation of a rare gas atom to an excited atomic state followed by an associative ionization collision process to form the molecular ion $(R_1R_2)^+$. However, R_1^* can radiate before it has a chance to collide with R_2; thus these experiments usually have to be carried out in a high pressure ion source. The accuracy of the appearance potentials obtained by electron beam excitation is always limited by

the energy spread of the beam, the threshold law for the electron
excitation process and finite kinetic energy possessed by the colliding
pair. From the photoionization experiments which were done in high
pressure gas cells without mass discrimination, Huffman et al.[1] and
Samson et al.[2] were able to obtain the lower bound of the dissociation
energies for the Xe_2^+, Kr_2^+ and Ar_2^+ symmetric rare gas molecular ions.
Owing to the lack of mass discrimination, their experimental technique
cannot be applied to nonsymmetric rare gas pairs.

Direct photoionization of rare gas van der Waals molecules offers
several attractive features. The formation of $(R_1R_2)^+$ could be
considered as a process in which initial photoexcitation of one of
the rare gas atoms in the dimer to an excited atomic Rydberg state
occurs followed by a nearly zero kinetic energy associative ionization
process. Since the dimer is just like a persistent weakly bound
colliding complex, the second step, which involves a vibrationally
induced autoionization process, is expected to be much faster than the
radiative decay of the excited rare gas atom. In other words, the
formation of $(R_1R_2)^+$ from van der Waals R_1R_2 dimer will almost proceed
with a unit quantum yield; thus the problem of the competition between
radiative decay and associative ionization process in the gas cell
experiment does not exist here. Furthermore, the excitation selection
rule for an atom in a dimer is also expected to relax as a consequence
of weak perturbation by its partner. Thus, the ionization potentials
of the dimers determined this way will not only be free from the
uncertainty of finite kinetic energy possessed by the colliding pair

as in conventional methods, but also the accuracy of the I.P. will

not be limited by the availability of dipole allowed transitions to

atomic levels near the threshold. The major drawbacks are the low

concentration of rare gas van der Waals dimers in the beam which

requires both an intense vacuum UV photon source and a sensitive

mass spectrometric detection system.

Recently, by combining the molecular beam technique with photo-

ionization mass spectrometry, our laboratory has been able to carry

out photoionization studies on the Xe_2,[3] Kr_2 and Ar_2[4] van der

Waals molecules. It was found that the formation of the symmetric

rare gas molecular ions involves mainly the autoionization process.

The autoionization of the rare gas dimers was found to obey the

parity selection rule $\Delta \ell = \pm 1$. In this work, we report the photo-

ionization studies of the heteronuclear rare gas van der Waals

molecules, XeKr, XeAr and KrAr.

EXPERIMENTAL

The experimental apparatus is essentially the same as that described

previously.[5,6] Briefly, the apparatus consists of a quadrupole mass

spectrometer, a modulated molecular beam production system, a windowless

1 m vacuum ultraviolet monochromator and a capillary discharge light source.

Depending on the spectral region, either the He Hopfield continuum or

the hydrogen many-line pseudocontinuum was used. The light intensity

was monitored by a sodium salicylate coated photomultiplier. The

spectrometer grating is gold coated, ruled with 1200 lines/mm and has a reciprocal dispersion of 8.3 Å/mm. Using 300 μm entrance and exit slits, the resolution achieved is 1.3 Å FWHM.

The XeKr, XeAr and KrAr molecules were prepared by supersonic expansion of the premixed rare gases through a 0.127 mm diameter nozzle with a stagnation pressure of ~400 torr for XeKr, and ~700 torr for XeAr and KrAr. In order to be able to maximize the formation of the heteronuclear rare gas van der Waals molecules during the expansion, the photoionization efficiency of the dimers at 800 Å for XeKr and 780 Å for XeAr and KrAr was measured for various proportions of the rare gases. It was found that the concentration of the hetero-nuclear dimers formed is very sensitive to the mixing ratio of the corresponding atoms at a given stagnation pressure, as is indicated by the results in Fig. 1. In view of the strong pressure dependence of the concentration of the dimers relative to that of the monomers in the expansion, the nozzle stagnation pressure had to be well regulated.

The beam of symmetric and asymmetric van der Waals molecules together with the corresponding rare gas atoms intersected the dispersed vacuum ultraviolet photon beam at a distance of 7.6 cm from the nozzle. The ions were focused and mass analyzed. With two stages of differential pumping, the main chamber maintained a pressure of ~5 x 10^{-7} torr during the experiment.

The monochromator was scanned automatically at 1 Å intervals, and at each wavelength the scalers were set to count for 100 to 800 sec depending on the counting rate at the particular spectral region. On

the average ion signals accumulated at a given point for XeKr, XeAr
and KrAr were 7000 ct, 3000 ct and 1500 ct respectively. For each
run, the photoionization efficiency of the van der Waals molecules
at a particular wavelength was arbitrarily chosen as a reference
point. From time to time, the monochromator was scanned back to the
reference point and the photoionization efficiency recorded, enabling
one to correct for fluctuations in the intensity of the dimer and
vacuum ultraviolet photon beams. It was found that the intensity
of the dimers remains constant to within 4%. The photoion spectra
reported in this work are the average of at least two scans. Wave-
length calibration was accomplished by using the emission lines of
the hydrogen atom and molecule as well as the atomic resonance lines
of He. The photon signal has been corrected for the background of
stray photons from the monochromator.

RESULTS AND DISCUSSION

A.   XeAr

The photoionization efficiency curve for XeAr is shown in Fig 2
and compared to the photoion spectra of Ar_2[4] and Xe. The ionization
potential obtained for XeAr is equal to 11.985 ± 0.017 eV. By combining
this with the I.P. of Xe[7] and the known binding energy for the XeAr van
der Waals molecule,[8] a value of 0.14 ± 0.02 eV for the dissociation
energy of the ground state diatomic molecular ion $XeAr^+$ is calculated.

The gross autoionization structure of the XeAr spectrum is consistent with the selection rule $\Delta\ell = \pm 1$ for both Xe and Ar, once good correlation is found between the Rydberg atomic levels derived from $5p^5(^2P_{1/2})ns$ (nd) for Xe, and $3p^5(^2P_{1/2, 3/2})ns$ (nd) for Ar, and the peaks in the XeAr spectrum. Autoionization structure coming from the excited atomic configuration $3p^5(^2P_{1/2, 3/2})5s$ (3d) of Ar, which was not observed in the photoion yield curve of Ar_2,[4] appeared as expected in the photoion spectrum of XeAr. One of the interesting results is that the Rydberg series $5p^5(^2P_{1/2})ns$ (nd) for Xe, which manifests itself as autoionization lines in the photoion spectrum of XeAr, is red shifted by about 3 Å with respect to the positions in the photoionization efficiency curve of Xe. Since the first excitation step is essentially a vertical process, this result suggests that the potential energies of the excited molecular Rydberg states formed by the interaction of Xe $(5p^5(^2P_{1/2})ns$ (nd)) and $Ar(^1S_0)$ at the equilibrium bond distance of ground state XeAr (4.1 Å)[8] are larger than the binding energy of the ground state van der Waals molecule XeAr. The shifts of the autoionization peaks, along with the known dissociation energy for XeAr (16.4 meV),[8] allows one to deduce the potential energies of these excited molecular Rydberg states at 4,1 Å. The experimental results are listed in Table I. The excited Xe atom essentially consists of an Xe^+ $(^2P_{1/2})$ core and a slow moving electron in a large excited atomic orbital; thus it is not unreasonable to assume the interaction potential for Xe^*-Ar to be dominated by the charge induced-dipole term. When the interaction distance is around 4.1 Å this estimate gives a

value of 0.04 eV as compared to the experimental value 0.06 eV (see Table I). Taking into account the uncertainty of this experiment (~0.017 eV) and the fact that only a point charge approximation is being used, the agreement is quite good. Similar agreement, as will be shown later, is found for all cases examined.

B. XeKr

The photoion spectrum of XeKr in the wavelength range from 800 to 1065 Å is depicted in Fig. 3. The photoion yield spectra of Kr_2[4] and Kr are also shown for comparison. The photoionization efficiency curve of the XeKr dimer increases quite quickly from the onset to 1050 Å as compared to that of Xe_2,[3] Kr_2 and Ar_2[4] near the threshold. In the wavelength region from 1050 to 1022 Å, the photoionization efficiency increases rather slowly. At 1012 Å (12.25 eV) there is a dramatic increase in the photoionization cross section due to the appearance of a strong autoionization peak. It is interesting to note that this value coincides with the previously suggested appearance potential for $(XeKr)^+$ as determined by electron impact mass spectrometric methods.[9,10] Since this value is slightly higher than the I.P. of Xe, Munson et al.[10] have suggested that the ground state of $(XeKr)^+$ is not bound. However, using the ionization potential of XeKr, 11.757 ± 0.017 eV, determined in this experiment, along with the I.P. of Xe[7] and the ground state dissociation energy of XeKr (20 meV)[11] as obtained from low energy elastic scattering of Kr on Xe, we deduce the binding energy between $Kr(^1S_0)$ and $Xe^+(^2P_{3/2})$ to be 0.37 ± 0.02 eV.

Analysis of the XeKr spectrum reveals good correlation of the autoionization structure with the atomic energy levels derived from the atomic configuration $4p^5(^2P_{1/2, 3/2})ns$ (nd) of Kr. Unlike the photoion spectrum of XeAr, the identification of the Rydberg series $5p^5(^2P_{1/2})ns$ (nd) of the Xe atom in this spectrum is not as obvious.

The comparison of the photoionization efficiency curves of XeKr and Kr show that the $4p^5(^2P_{1/2})ns$ (nd) atomic lines of Kr are red shifted in the XeKr spectrum. Using the known binding energy of the XeKr van der Waals molecules (20 meV),[11] the potential energy of these excited molecular Rydberg states as derived by the combination of a normal $Xe(^1S_0)$ atom and an excited Kr $4p^5(^2P_{1/2})ns$ (nd) atom at the equilibrium interatomic distance of ground state XeKr (4.19 Å)[11] is calculated as 0.10 eV. The charge induced-dipole approximation yields a value of 0.09 eV, again in good agreement with the experimental value. See Table II.

Similar autoionization structure attributed to the Rydberg series $4p^5(^2P_{1/2})ns$ (nd) of Kr can also be identified in the photoion yield curve of Kr_2 obtained previously.[4] Table III lists the experimental value of the potential energy of Kr $4p^5(^2P_{1/2})ns$ (nd) + $Kr(^1S_0)$ at the equilibrium interatomic distance of Kr (4.006 Å)[12] as 0.09 eV, while the charge induced-dipole term gives an estimate of 0.07 eV.

C. KrAr

The photoionization efficiency curve of KrAr is shown in Fig. 4. The threshold for photoionization of KrAr is 923.5 ± 1.5 Å which

corresponds to an ionization potential of 13.425 ± 0.020 eV. Using

the binding energy for KrAr (14.9 meV),[8] the binding energy for $KrAr^+$

is calculated as 0.59 ± 0.02 eV.

In the spectral regions from 923.5 Å (I.P. of KrAr) to 886 Å

(I.P. of Kr)[7], and 853 Å (I.P. of Ar_2)[4] to 786 Å (I.P. of Ar)[7], the

autoionization structure is very similar to that which appeared

in the photoion spectra of Kr_2 and Ar_2,[4] respectively. In the

region ~860 - 890 Å where both Kr and Ar have excited atomic Rydberg

levels derived from the $n'p^5ns$ (nd) configuration (where n' = 4

for Kr, and n' = 3 for Ar), the autoionization structure arising from

the atomic lines of Ar seems to predominate. This conclusion is

suggested by the observation of similar autoionization structure in

the photoionization efficiency curves of both XeAr and KrAr in this

region. Nevertheless, a careful examination also indicates blue

shifts of the auotionization peaks observed in the photoion spectrum

of KrAr relative to those resolved in the spectrum of XeAr. Attempts

have been made to resolve the autoionization structure coming from

individual atomic lines. Higher resolution runs in this portion of

the spectra have been carried out for KrAr and XeAr. The spectra

obtained with 100 μm entrance and exit slits (three times better

resolution) are depicted and compared in Fig. 5. The FWHM of the

autoionization peaks shown in these spectra are still wide (≥ 2.5 Å),

about the same as those resolved in the previous spectra. Good

correlation is found between the atomic levels of Ar and the position

of the autoionization peaks observed in XeAr. Assuming that the

autoionization peaks in KrAr and XeAr arise from similar molecular

Rydberg states, the Rydberg states in KrAr apparently have potential

humps around the van der Waals radius of ground state KrAr (3.9 Å).

Maxima in the potential energy curves of states whose Rydberg mole-

cular orbitals are of a promoted type[13] have been discussed by

Mulliken for the heavy rare gas dimers.[14]

CONCLUSION

The ionization potentials of the heteronuclear rare gas dimers

XeKr, XeAr and KrAr as well as the binding energies of these

heteronuclear molecular ions deduced in this experiment are

summarized and compared to the appearance potentials obtained by

electron impact mass spectrometric methods in Table IV. The

dissociation energies of the ground state asymmetric rare gas

dimeric ions are found to be much smaller than those of the

symmetric rare gas diatomic molecular ions.

In general, the autoionization of XeKr, XeAr and KrAr is found

to obey the parity selection rule $\Delta \ell = \pm 1$ which is in agreement

with the autoionization mechanism observed in the photoionization

studies of Kr_2 and Ar_2. In order to further elucidate and rationalize

this observation, schematic representations of $R_1 + R_2$, $R_1^* + R_2$ and

$R_1^+ + R_2$ potential energy curves are shown in Fig. 6. The ground

state of the van der Waals molecule $R_1 R_2$ has a very shallow

well at ~4 Å. However, the ground molecular-ionic

state of $(R_1R_2)^+$ is bound and has an equilibrium bond distance of

~2.5 Å. As mentioned before, autoionization essentially consists

of two discrete steps, i.e.

$$R_1 \cdots R_2 + h\nu \xrightarrow{(1)} R_1^* \cdots R_2 \text{ (or } R_1 \cdots R_2^*) \xrightarrow{(2)} (R_1R_2)^+ + e$$
$$\xrightarrow{(3)} R_1 \cdots R_2 + h\nu'$$

The first step (1) is the excitation of the dimer R_1R_2 to a resonant

molecular Rydberg state having a Rydberg electron in an excited atomic

orbital associated entirely with the excited atom, R_1^* (or R_2^*). The

second step (2) is the interaction between the excited Rydberg electron

and the ion core which results in the ejection of the electron and

formation of $(R_1R_2)^+$ in a discrete ionic level. If the second step (2)

is much faster than the radiative decay (3) of the excimer, the first

excitation step (1) will be the rate determining process. In the

dissociation limit, the excitation process will be totally governed

by the atomic excitation selection rule, i.e, $\Delta \ell = \pm 1$, $\Delta J = 0, \pm 1$. In

the molecular case, the selection rule, according to Hund-Mulliken's

case (c) is $\Delta \Omega = 0, \pm 1$.[15] Since the van der Waals ground state is a

0^+ state, transitons from 0^+ to 0^+ or 1 excited molecular states are

the only ones which are dipole allowed. However, all the excited

atomic states (except those with J = 0) can couple with the ground

state R_2 atom $(^1S_0)$ to give a 0^+ and/or 1 molecular state. Thus,

all excited atomic levels, including those derived from atomic

configurations $n'p^5(^2P_{1/2,\ 3/2})np$ (nf) (where n' = 3 for Ar,

n' = 4 for Kr and n' = 5 for Xe) having energy higher than the minimum

of the ground state potential energy curve of the molecular ion, $(R_1 R_2)^+$, are available for autoionization. Our experiment samples the excitation processes at the region of the van der Waals radius and the results suggest an excitation selection rule $\Delta \ell = \pm 1$, which is somewhat between the molecular and atomic cases.

-13-

REFERENCES

1.   R. E. Huffman and D. H. Katayama, J. Chem. Phys., 45, 138 (1966).

2.   J. A. R. Samson and R. B. Cairns, J. Opt. Soc. Am., 56, 1140 (1966).

3.   C. Y. Ng, D. J. Trevor, B. H. Mahan and Y. T. Lee, J. Chem. Phys., 65, 4327 (1976).

4.   C. Y. Ng, D. J. Trevor, B. H. Mahan and Y. T. Lee, J. Chem. Phys., to be published.

5.   C. Y. Ng, B. H. Mahan and Y. T. Lee, J. Chem. Phys., 65, 1956 (1976).

6.   C. Y. Ng, Ph.D. Thesis, The University of California, Berkeley (1976).

7.   C. E. Moore, Atomic Energy Levels, NBS Circ., 467, Vol. I, II and III (1949).

8.   J. M. Parson, T. P. Schaefer, P. E. Siska, F. P. Tully, Y. C. Wong, and Y. T. Lee, J. Chem. Phys., 53, 3755 (1970).

9.   W. Kaul and R. Taubert, Z. Naturforsch., 179, 88 (1962).

10.   M. S. Munson, J. L. Franklin and F. H. Field, J. Phys. Chem., 67, 1542 (1963).

11.   R. J. Buss, C. H. Becker and Y. T. Lee, J. Chem. Phys., to be published.

12.   J. A. Baker, R. O. Watts, J. K. Lee, T. P. Schaefer and Y. T. Lee, J. Chem. Phys., 61, 308 (1974).

13.   R. S. Mulliken, Phys. Rev., 136, A962 (1964).

14.   R. S. Mulliken, J. Chem. Phys., 52, 5170 (1970).

15.   R. S. Mulliken, Rev. Mod. Phys., 3, 89 (1931); 4, 1 (1932).

Table I. Potential Energy of Xe*-Ar at the van der Waals Radius of XeAr.

Xe Atomic Lines $\lambda(\overset{\circ}{A})$	Atomic Autoionization peak observed in the P.E. curve of Xe ($\overset{\circ}{A}$)	Corresponding Peaks position observed in the P.E. curve of XeAr ($\overset{\circ}{A}$)	Potential energy of Xe*-Ar at the van der Waals radius	Charge-induced dipole interaction (Xe$^+$-Ar) at the van der Waals radius
$6d'[1\frac{1}{2}]^0_1$ 995.84	995.0	998.5	− 0.06 eV	− 0.04 eV
$8s'[\frac{1}{2}]^0_1$ 985.9	986.5	989.5	− 0.06 eV	
$7d'[1\frac{1}{2}]^0_1$ 966.94	966.5	969.5	− 0.06 eV	
$8d'[1\frac{1}{2}]^0_1$ 952.12	951.5	954.5	− 0.06 eV	
$9d'[1\frac{1}{2}]^0_1$ 943.7	943.5	946.5	− 0.06 eV	

Parameters for the ground state XeAr potential[a]

ϵ = 16.4 meV

r_m = 4.10 $\overset{\circ}{A}$

(a) Reference 8

-14-

Table II. Potential Energy of Xe-Kr* at the van der Waals Radius of XeKr.

Kr Atomic Lines $\lambda(\text{Å})$	Atomic Autoionization peak position observed in the P.E. curve of Kr (Å)	Corresponding peak position observed in the P.E. curve of KrXe (Å)	Potential Energy of Xe-Kr* at the van der Waals radius	Charge-induced dipole interaction (Xe-Kr*) at the van der Waals radius
6d'$[1\tfrac{1}{2}]^0_1$ 881.06	880.5	885.5		
8s'$[\tfrac{1}{2}]^0_1$ 879.4			-0.10 eV	-0.09 eV
7d'$[1\tfrac{1}{2}]^0_1$ 869.5	869.0	874.5		
9s'$[\tfrac{1}{2}]^0_1$ 868.6			-0.11 eV	
8d'$[1\tfrac{1}{2}]^0_1$ 862.7	862.5	867.5		
10s'$[\tfrac{1}{2}]^0_1$ 862.4			-0.10 eV	
9d'$[1\tfrac{1}{2}]^0_1$ 858.52	858.5	863.5		
11s'$[\tfrac{1}{2}]^0_1$ 858.2			-0.10 eV	
10d'$[1\tfrac{1}{2}]^0_1$ 857.7	855.0	860.5		
12s'$[\tfrac{1}{2}]^0_1$ 855.0			-0.11 eV	

Parameters for the ground state XeKr potential[a]

ϵ = 20 meV

r_m = 4.19 Å

(a) Reference 11

Table III. Potential Energy of Kr*-Kr at the van der Waals Radius of Kr$_2$

Kr Atomic Lines λ(Å)		Atomic Autoionization peak position observed in the P.E. curve of Kr (Å)	Corresponding peak position observed in the P.E. curve of Kr$_2$ (Å)	Potential energy of Kr*-Kr at the van der Waals radius	Charge-induced dipole interaction (Kr$^+$-Kr) at the van der Waals radius
$6d'[1\frac{1}{2}]^0_1$	881.06	880.5	885.0		
$8s'[\frac{1}{2}]^0_1$	879.4			-0.09 eV	-0.07 eV
$7d'[1\frac{1}{2}]^0_1$	869.5	869.0	874.0		
$9s'[\frac{1}{2}]^0_1$	868.6			-0.10 eV	
$8d'[1\frac{1}{2}]^0_1$	862.7	862.5	867.0		
$10s'[\frac{1}{2}]^0_1$	862.4			-0.09 eV	

Parameters for the ground state Kr$_2$ potential[a]

ϵ = 17.4 meV

r_m = 4.0060 Å

(a) Reference 12
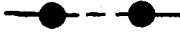
Table IV.   Ionization Potentials and Dissociation Energies of the Heteronuclear Rare Gas Dimers
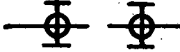
	Ionization Potentials of the Heteronuclear Rare Gas Dimer (eV)			Dissociation of the Heteronuclear Rare Gas Ion (eV)
	Electron Impact		Photoionization (this work)	Photoionization (this work)
	(a)	(b)		
XeKr$^+$	12.3 ± 0.1	12.2	11.757 ± 0.017	0.37
XeAr$^+$	13.5 ± 0.1	13.5	11.985 ± 0.017	0.14
KrAr$^+$	14.0 ± 0.1		13.425 ± 0.02	0.59

(a)   Reference 10

(b)   Reference 9

FIGURE CAPTIONS

Fig. 1. ——●——●—— Relative intensity of XeKr versus

[Kr]/[Xe] measured at 800 Å.

——⊕——⊕—— Relative intensity of XeAr versus

[Ar]/[Xe] measured at 780 Å.

——■——■—— Relative intensity of KrAr versus

[Ar]/[Kr] measured at 780 Å.

Fig. 2. Photoionization efficiency curve of XeAr in the wavelength

range from 800 to 1045 Å as compared to the photoionization

efficiency curves of Xe, Ar and Ar_2.

Fig. 3. Photoionization efficiency curve of XeKr in the wavelength

range from 800 to 1065 Å as compared to the photoionization

efficiency curves of Kr and Kr_2.

Fig. 4. Photoionization efficiency curve of KrAr in the wavelength

range from 790 to 930 Å as compared to photoionization

efficiency curves of Kr, Ar, Kr_2 and Ar_2.

Fig. 5. Higher resolution photoionization efficiency curves of XeAr

and KrAr in the wavelength range from 860 to 895 Å.

Fig. 6. Schematic representation of potential energy curves of

$R_1 + R_2$, $R_1^* + R_2$ and $R_1^+ + R_2$ (where R_1 (or R_2), R_1^* and

R_1^+ are rare gas atoms, an excited rare gas atom and an atomic

rare gas ion respectively).
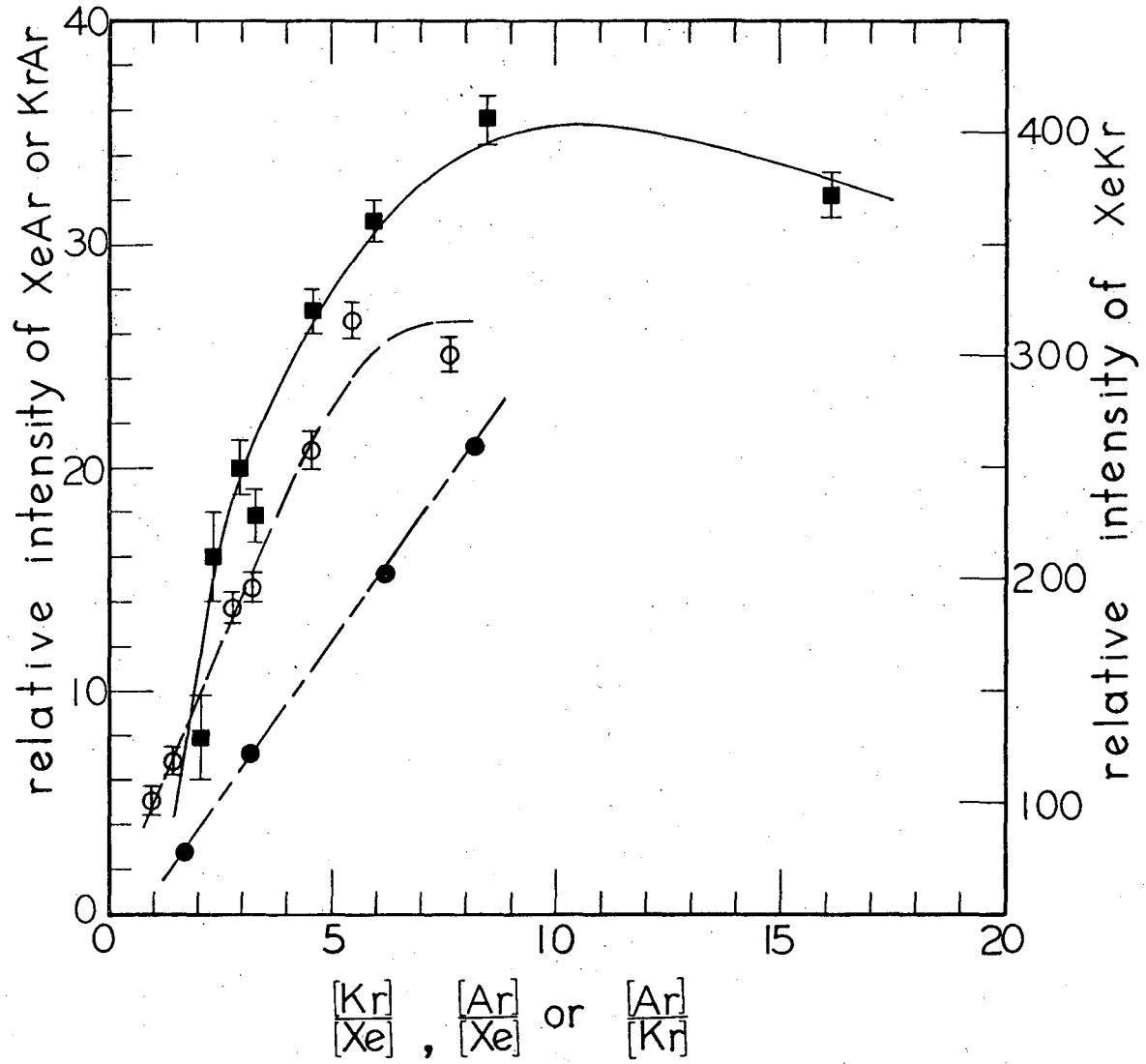
XBL 7612-10879

Fig. 1
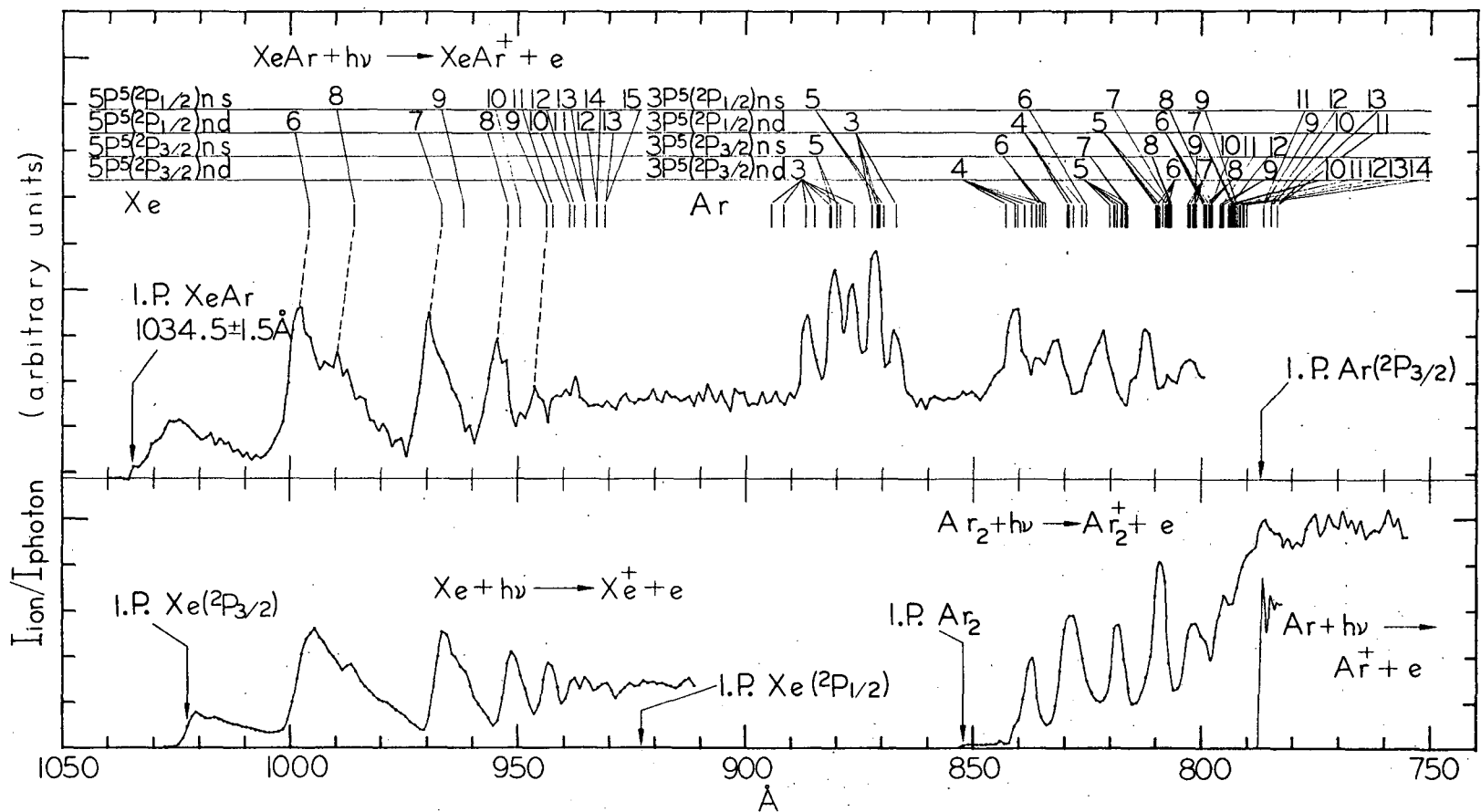
Fig. 2
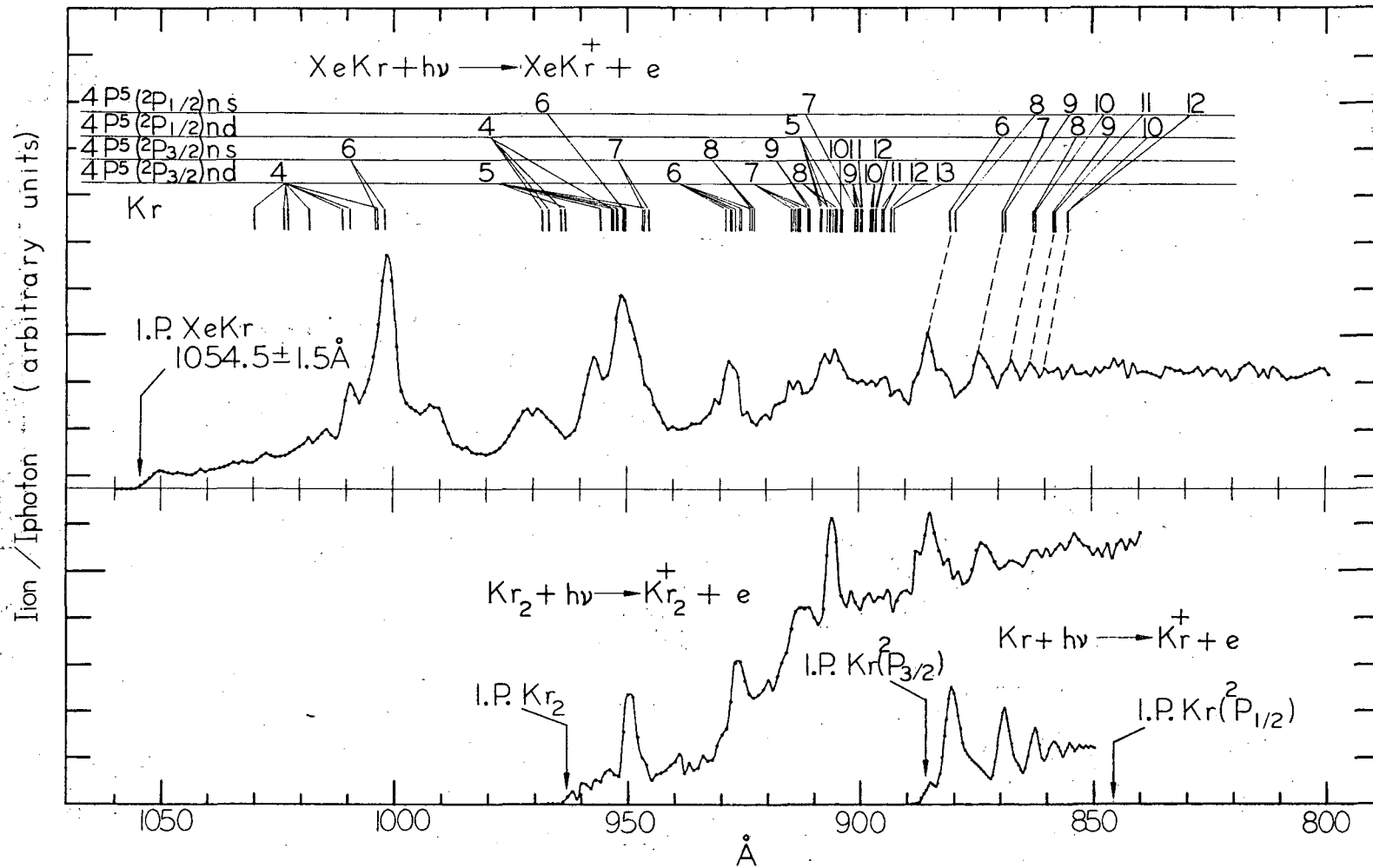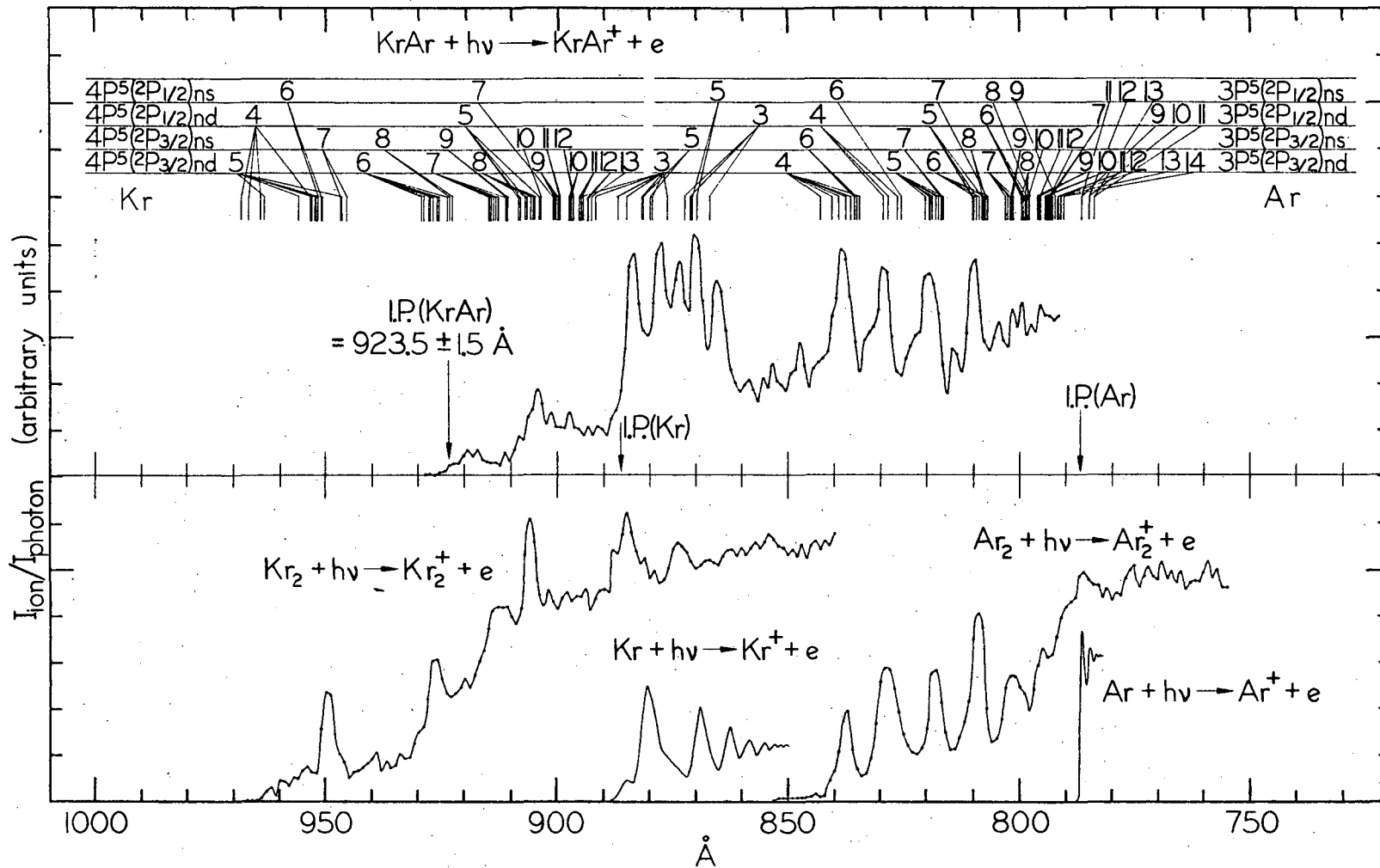
Fig. 3

XBL 7612-10876

Fig. 4

XBL 7612-10875

Fig. 5

XBL 7612-10878

Fig. 6

XBL 771-7241